Miscibility Study of Stereoregular Poly(methyl methacrylate) Blends. Experimental Determination of Phase Diagrams and Predictions

L. Ragupathy, V. Arrighi,* J. M. G. Cowie, R. Ferguson, and I. J. McEwen

Chemistry, School of Engineering and Physical Sciences, Heriot-Watt University, Edinburgh EH14 4AS, U.K.

S. L. Shenoy†

Chemical and Life Sciences Engineering, Virginia Commonwealth University, 601 West Main Street, P.O. Box 843028, Richmond, Virginia 23284-3028

Received July 19, 2006; Revised Manuscript Received December 15, 2006

ABSTRACT: Miscibility behavior of blends of isotactic and syndiotactic poly(methyl methacrylate) (iPMMA and sPMMA) was investigated as a function of annealing temperature and molecular weight of the iPMMA component. Annealing experiments clearly indicate that for the high molecular weight iPMMA sample formation of stereocomplexes between isotactic and syndiotactic PMMAs is hindered. Annealing experiments carried out in the temperature range 313−473 K, followed by DSC measurements, showed that iPMMA is completely miscible with sPMMA only in a narrow temperature range around 350 K. To explain these experimental data, a simple theoretical model for the prediction of phase behavior of polymer blends involving dispersive interactions, is presented. This model accounts for subtle structural differences (e.g., stereoisomerism) between the repeat units of the blend components, and by incorporating the surface to volume ratios into the original Flory−Huggins solubility parameter approach, which makes it possible to account for packing effects on blend miscibility. The model is able to predict the presence of both UCST and LCST experimentally observed for stereoregular PMMA blends, without employing an equation of state approach.

1. Introduction

Over the past few years several reports on miscibility of polymer blends in which the components differ only in stereochemical compositions have been published.[1−7] For example, the miscibility behavior of stereoregular blends of polypropylene[1−3] and polystyrene[4−6] has been extensively studied. We have recently carried out measurements on blends of head-to-head polypropylene with conventional head-to-tail atactic, syndiotactic and isotactic polypropylenes.[7] The main interest in these systems stems from the fact that, since the blend components have identical repeat units, a variation in the phase behavior is solely a consequence of microstructural differences between the blend components.

The miscibility behavior of isotactic/ syndiotactic poly(methyl methacrylate) (iPMMA/sPMMA) has also generated considerable interet.[8−10] A unique feature of this blend system is the large difference between the glass transition temperature of the isotactic and syndiotactic structures (T_g of iPMMA $\approx$ 333 K and T_g of sPMMA $\approx$ 408 K). Thus, in principle, one can employ differential scanning calorimetry (DSC) to investigate blend miscibility. However, contrasting results have been reported in the literature.

Using dilatometry, Krause and Roman[8] reported that isotactic PMMA is miscible with the syndiotactic form while Bauer and Bletso,[9] based on dilatometry, mechanical damping, and torsional modulus data, reached the conclusion that iPMMA/ heterotactic PMMA blends are immiscible. DSC measurements carried out by Schroeder et al.[10] indicated that when iPMMA and sPMMA samples of comparable molecular weight are mixed, miscible systems form at all compositions. By performing annealing experiments, these authors concluded that the lower critical solution temperature (LCST) of these blends was located above the degradation temperature of PMMA.

As reported by various authors, stereocomplexation between iPMMA and sPMMA adds further complexity to any study of miscibility behavior in stereoregular PMMA blends.[11−18] The idea of stereospecific interaction between isotactic and syndiotactic PMMAs was first proposed by Liquori et al.[11] Later, several studies were devoted to a better understanding of the nature and structure of the stereocomplex. For example, Bosscher et al.[13] suggested that the ester group of the isotactic chain and the α-methyl group of the syndiotactic chains are involved in the process of complexation.

Particular attention has been paid to the determination of the experimental conditions that favor association in solution and in bulk. These studies are particularly relevant when dealing with blends of steroisomeric PMMAs that may form stereocomplexes depending on temperature, molecular weight and/ or solvent.

It was found by Challa and co-workers[12] that the nature of the solvent has considerable impact on complex formation. Solvents for PMMA can be divided into three categories: those strongly complexing (e.g., acetone and tetrahydrofuran); those weakly complexing (e.g., toluene and benzene); and noncomplexing (e.g., chloroform and dichloromethane). Other factors, such as temperature, polymer concentration, mixing ratio of the stereoregular polymers, and contact time may also influence the formation of stereocomplexes between iPMMA and sPMMA.

DSC studies of the stereocomplexes have shown that annealing in the temperature range 403−433 K produces a melting endotherm on subsequent heating at about 463 K, even with samples precipitated from a noncomplexing solvent.[14] However

* To whom all correspondence should be addressed. E-mail: v.arrighi@hw.ac.uk. Telephone: +44 131 451 3108.

† Current address: Philip Morris USA Research Center, 4201 Commerce Road, Richmond, VA 23234.

10.1021/ma061627q CCC: $37.00
Published on Web 01/31/2007

Table 1. Characteristics of PMMA Samples Used in This Work

polymer	M_w/g mol^{-1}	M_w/M_n	T_g/K	tacticity
sPMMA	85 100	1.14	408	≈88% rr
iPMMA1	300 000	1.66	342	≈74% mm
iPMMA2	100 000	1.14	334	≈90% mm
iPMMA3	48 000	1.22	329	≈90% mm

the formation of a complex in bulk is a less favorable process than complexation in dilute solution since the maximum degree of crystallinity measured for the former is half the value found in solution prepared complexes.

Schomaker and Challa[15] investigated the process of stereocomplexation between isotactic and syndiotactic PMMA in the bulk, as a function of annealing temperature, annealing time and molar mass using DSC and WAXS. At low annealing temperatures (≈383 K), the authors observed multiple endotherms with different characteristics. The same authors also performed annealing experiments at 413 K as a function of the iPMMA (weight-average molar mass, M_w equal to 3.2×10^{-4} and 7.4×10^{-5} g mol^{-1}) and sPMMA molar mass ($M_w = 8.5 \times 10^{-4}$ and 6.2×10^{-5} g mol^{-1}) and concluded that low molar mass is necessary for complexation, favoring chain mobility. However, a systematic study of stereocomplexation and how this is affected by changing the molecular weight of one of the blend components, e.g., iPMMA, has yet to be performed.

Recently, Lemieux et al.[18] while investigating the crystallization behavior of the stereocomplexes as a function of annealing temperature, observed two distinct glass transitions corresponding to the T_gs of the pure components. This led to the conclusion that an heterogeneous phase is formed, as indicated by the two T_gs.

While contradictory reports have appeared on the phase behavior of iPMMA/sPMMA blends, one should note that this contradiction may be due to differences in the sample's molar mass or its tacticity, often not reported.

In this paper, we investigate systematically the miscibility behavior of narrowly distributed iPMMA/sPMMA blends as a function of annealing temperature and iPMMA molar mass. Thus, the phase behavior of 50/50 wt % blends of low, medium and high molecular weight isotactic PMMA blended with sPMMA is investigated using DSC and dynamic mechanical thermal analysis (DMTA).

The experimental data are compared with theoretical predictions from a newly developed, simple theoretical model which is described in this paper, for the first time.

2. Experimental Section

2.1. Materials. The iPMMA1 sample was purchased from Polysciences and used as received while iPMMA2 and iPMMA3 were obtained by fractionating a iPMMA sample from Polysciences. The sPMMA sample was kindly supplied by Professor Julia Higgins (Imperial College, U.K.). Sample tacticities (%) were determined by ^{13}C NMR measurements at 373 K, using a 400 MHz Bruker spectrometer (Table 1). Polymer solutions for ^{13}C NMR measurements were prepared in deuterated tetrachloroethylene.

2.2. Molecular Weight Determination. Polymer molecular weights were determined by gel permeation chromatography (Waters) in THF solution using two Polymer Laboratories 5μ mixed-C columns operating at a flow rate of 1.0 mL min^{-1}. Calibration was performed by narrow molecular weight polystyrene (PS) standards. Values of weight-average molar mass, M_w, and polydispersity are given in Table 1.

2.3. Blend Preparation. For iPMMA/sPMMA blends, the choice of solvent is critical in minimizing the possibility of stereocomplex formation between the stereoisomers. As a result, dichloromethane was employed as the solvent for blend preparation.[12] The resulting solution was coprecipitated by dropwise addition to a nonsolvent (petroleum ether). The precipitated polymer was dried in a vacuum oven at room temperature for 3 days to ensure complete solvent removal.

2.4. DSC Measurements. Glass transitions (T_g) were determined using a TA Instruments DSC 2010 with both heat flow and temperature scales calibrated against indium metal. Nitrogen was used as purge gas and samples were scanned at 20 °C min^{-1}. All T_g values listed in Table 1 refer to the midpoints of the inflection in the DSC traces.

For the blends, prior to the DSC measurements, samples were heated above the melting point of the stereocomplex (363 K) for 20 min, and this was followed by quenching to the desired annealing temperature. This procedure was adopted for all samples, including the pure components. The same sample was used for all annealing experiments.

2.5. DMTA Measurements. Three DMTA measurements were carried out on the iPMMA2/sPMMA blend. A sample was prepared by melt pressing at 473 K to prevent stereocomplex formation, and it was annealed for half an hour at $T = 473$ K and then quenched to room temperature. Three different samples were then cut from this initial film for the subsequent DMTA measurements. One of the samples was measured as prepared whereas the other two samples were annealed at 353 and 313 K, respectively, for 12 h. After annealing, they were quenched to room temperature and used for DMTA measurements. A typical sample size was 1.2 cm × 1 cm × 0.08 cm. Single cantilever DMTA measurements were carried out using a heating rate of ∼2 K/min and a frequency of 1 Hz.

3. Theoretical Model

The theoretical model developed here is based on the idea proposed by Staverman that differences in segmental surface areas of the components are of utmost importance to correctly predict phase behavior of mixtures of small molecules.[19] As detailed below, Staverman's idea is here incorporated into the classical Flory−Huggins (FH) theory and therefore extended to polymer mixtures.

The traditional FH theory is frequently employed in calculations of polymer−polymer phase diagrams. The Gibbs free energy of mixing is given by the well-known expression[20]

$$\Delta G_m = \frac{\varphi_1 \ln \varphi_1}{m_1} + \frac{(1-\varphi_1)\ln(1-\varphi_1)}{m_2} + \chi\varphi_1(1-\varphi_1) \quad (1)$$

where φ_1 is the volume fraction and m_i the number of repeating units in each polymer chain i. χ is the FH interaction parameter which can be estimated from BV_{ref}/RT, where B is the solubility parameter difference $(\delta_1 - \delta_2)$,[2] V_{ref} is the reference volume, R is the gas constant, and T is the temperature.

Various factors such as chain connectivity,[21] chain stiffness,[22] free volume,[22,23] and interactions between blend components[24] are known to contribute to the Gibbs free energy of mixing, leading to nonideality. Traditionally, these effects have been collectively accounted for in some manner, for example, by making χ both temperature and composition dependent. Thus, for a reasonably accurate prediction of blend phase behavior both temperature and composition dependence of the dominant factors affecting χ must be included in eq 1.

3.1 Relationship between Solubility Parameter Difference $[(\delta_1 - \delta_2)^2]$ and Surface to Volume Ratio (s). The FH theory is able to predict miscibility due to apparent energetic interactions but it neglects packing effects. In order to describe the effect of packing on enthalpy due to structural variations (e.g., stereo and structural isomerism), the solubility parameter difference B can be related to the surface to volume ratios

(s = surface/volume) of the corresponding molecules, s_1 and s_2, in the mixture by using the van Laar heat of mixing.[25]

$$\frac{\Delta H_m}{\varphi_1(1-\varphi_1)} = \left[\delta_1\left(\frac{s_2}{\bar{s}}\right)^{1/2} - \delta_2\left(\frac{s_1}{\bar{s}}\right)^{1/2}\right]^2 \quad (2)$$

where $\bar{s} = s_1\varphi_1 + s_2(1-\varphi_1)$.

Since the term on the RHS of eq 2 represents the solubility parameter difference B, if we define $\nu = s_1/s_2$ and rearrange, we obtain

$$B = \frac{(\delta_1 - \delta_2\sqrt{\nu})^2}{\varphi_1\nu + (1-\varphi_1)} \quad (3)$$

3.2. Relationship between *s* and Chain Conformation. The surface to volume ratio can be calculated using the Bondi's[26] group contribution method. For polymers, s calculated in this manner will not reflect the effect of the surrounding environment or chain size. Hence, it is necessary to incorporate the influence of the surrounding molecular environment on s, and here we introduce a definition based on the random coil conformation of the polymer chains

$$s = \frac{4\pi R_g^{\,2}}{V} \quad (4)$$

where R_g is the radius of gyration of the polymer chain and V the corresponding volume.

The radius of gyration, R_g, is identified with the unperturbed chain dimension and is defined in terms of the Kuhn segment length, which is in turn related to the characteristic ratio, C_∞. Coincidentally, this definition of s is closely related to the structural parameter $\beta^2 = R_g^2/V$ defined by Helfand and Sapse.[27]

For defining chain conformation quantitatively, it is convenient to conform to the procedure of Wu who has identified elementary rotational units for a large number of polymers.[28,29] Hence, using Wu's analysis, the radius of gyration of a real chain can be written as follows:

$$R_g^{\,2} = \frac{1}{6}C_\infty n\langle l_v\rangle^2 = \frac{1}{6}b_k n\langle l_v\rangle \quad (5)$$

where b_k ($= C_\infty\langle l_v\rangle$) is the Kuhn length, n is the number of elementary or statistical skeletal units in a chain, and $\langle l_v\rangle^2$ is the mean square length of a statistical skeletal unit. Subtle changes in the structure of the elementary units can alter C_∞ (and hence R_g, thus affecting s and so the phase behavior).

Using eqs 4 and 5 and the definition of Kuhn segment volume $V_b = Vb_k/nl_v$, where V is the volume of the polymer chain, the surface to volume ratio in the bulk can be defined as follows.

$$s = \frac{2\pi b_k^{\,2}}{3V_b} \quad (6)$$

By considering a cylindrical unit ($V_b = \pi r^2 h$) of length b_k and diameter d, it follows that

$$s = \frac{8b_k}{3d^2} \quad (7)$$

Using these relationships, from the solubility parameter difference to the characteristic ratio, and applying the spinodal condition ($\partial^2\Delta G_{mix}/\partial\varphi_i^2 = 0$), a phase diagram of temperature (T) vs volume fractions (φ_1) can be generated.

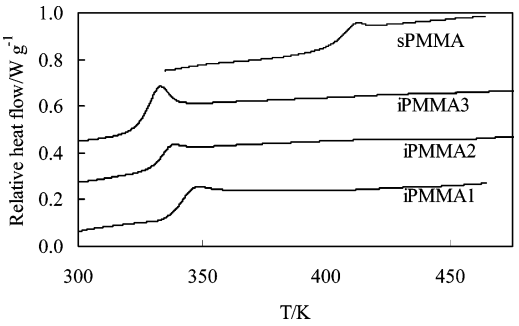

Figure 1. DSC thermograms of pure PMMAs. Each trace is displaced vertically for clarity.

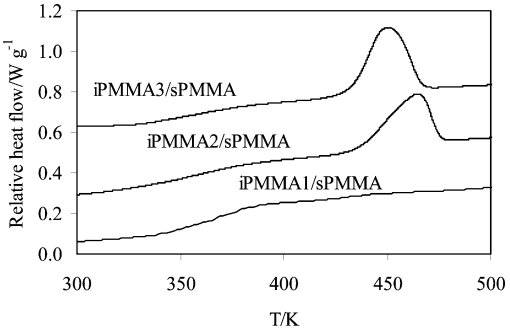

Figure 2. Effect of molecular weight on stereocomplex formation for 50/50 iPMMA/sPMMA blends annealed at 408 K. Each trace is displaced vertically for clarity.

Table 2. Endothermic Peak Characteristics of iPMMA/sPMMA Samples after Annealing at 408 K

blends	T_m/K	ΔH_m/J g^{-1}
iPMMA3/sPMMA	449	22
iPMMA2/sPMMA	463	20
iPMMA1/sPMMA		
30 h	461	4
3 days	466	6
14 days	468	9

4. Results and Discussion

Figure 1 shows the DSC traces of iPMMA1, iPMMA2, iPMMA3, and sPMMA. The midpoint T_gs of iPMMAs and sPMMA were observed to be in the range 330−340 K and at 408 K, respectively (Table 1) and so results are in good agreement with values reported in the literature.[18] It is likely that the higher T_g value for iPMMA1 may be due to the lower isotacticity of this sample compared to iPMMA2 and iPMMA3.

4.1. Formation of Stereocomplexes in iPMMA/sPMMA Blends. The optimum temperature for formation of a stereocomplex between isotactic and syndiotactic PMMA is 408 K, as reported by Feitsma et al.[14] Figure 2 gives the DSC scans for 50/50 wt % blends of iPMMA1/sPMMA, iPMMA2/sPMMA, and iPMMA3/sPMMA, annealed at 408 K for 12 h. As shown in Figure 2, the large endothermic peak observed at ~460 K for the iPMMA2/sPMMA and iPMMA3/sPMMA samples corresponds to melting of the stereocomplexes.[15] Values of the endothermic peak maxima and ΔH_m (associated with at least a ±5% uncertainty) are listed in Table 2. They are in good agreement with literature data.[14,15]

Because of the presence of a large endothermic peak, all glass transitions are ill defined, in a similar way to semicrystalline polymers where the glass transition is often barely discernible in the DSC trace, due to high levels of crystallinity.

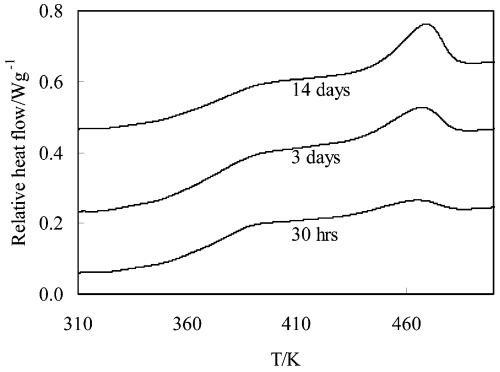

Figure 3. Effect of annealing time on a 50/50 iPMMA1/sPMMA samples, at 408 K. Each trace is displaced vertically for clarity.

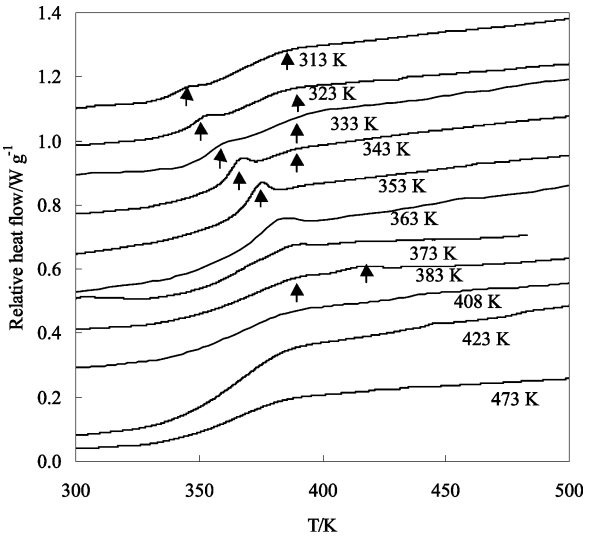

Figure 4. DSC thermograms of 50/50 iPMMA1/sPMMA blends as a function of annealing temperature. Arrows indicate thermal transitions and each trace is displaced vertically for clarity.

Surprisingly, no endothermic peak is observed for the iPMMA1/sPMMA sample after 12 h annealing, suggesting that the high molecular weight iPMMA1 does not form stereocomplexes with sPMMA. However, after increasing annealing time to 30 h, a small endothermic peak was observed at ~460 K. The intensity of this peak further increases upon annealing for 3 and 14 days (Figure 3). The peak maxima and the estimated ΔH_m values are given in Table 2.

These observations are consistent with work of Schomaker and Challa[15] who reported that high M_w hinders the lamellar crystallization of the stereocomplexes when annealing at 413 K. In the present study, the M_w of the iPMMA sample is 3.5 times higher than that of sPMMA, which might explain why the stereocomplexation does not take place during short annealing times (~12 h).

4.2. Miscibility Studies of 50/50 iPMMA1/sPMMA. Figure 4 shows the DSC traces obtained after annealing the 50/50 wt % iPMMA1/sPMMA blend from 313 to 473 K (T_{ann}). The observed midpoint T_g together with the ΔT values, corresponding to the difference between T_g onset and final, are given in Table 3.

For annealing temperatures, $T_{ann,}$ in the range 313−343 K, stereocomplexation is negligible as indicated by the absence of the endothermic peak around ~460 K in Figure 4. In addition, the blends exhibit two T_gs indicating phase separation of the iPMMA1 and sPMMA components. With increasing T_{ann} from 313−343 K, the difference between T_gs decreases and this is accompanied by decreasing ΔT values for T_{g2} (Table 3). These results suggest that miscibility of iPMMA with sPMMA increases gradually when increasing T_{ann} from 313 to 343 K.

Table 3. T_g and ΔT Values Obtained after Annealing 50/50 iPMMA1/sPMMA Blend Samples

	T_{g1}/K		T_{g2}/K	
T_{ann}/K	T_g	ΔT	T_g	ΔT
313	342	11	364	27
323	350	10	373	22
333	349	10	375	23
343	363	10	381	10
353	371	10		
363	377	18		
373	367	35		
383	374	41	406	8
408	373	40		
423	366	36		
473	373	27		

At T_{ann} = 353 K, a single T_g (=371 K) is observed with a small ΔT of 10, clearly indicating that iPMMA is completely miscible with sPMMA. This is in good agreement with the calculated T_g value (373 K) using the Flory−Fox equation[31]

$$\frac{1}{T_{g12}} = \frac{w_1}{T_{g1}} + \frac{w_2}{T_{g2}} \tag{8}$$

where w_1 and w_2 are the weight fractions of the blend components with glass transitions T_{g1} and T_{g2}, respectively, and T_{g12} is the blend glass transition. Flory−Fox behavior is typically expected for one-phase systems with little or no interaction between the components.

Similar results were obtained on annealing at 363 and 373 K, but in this case the observed breadth of the T_g values was 18 and 35 K respectively, suggesting that samples are only marginally miscible at these temperatures. But, Lemieux and Prud'homme[18] observed two T_gs at these annealing temperatures (363 and 373 K) and concluded that iPMMA and sPMMA are immiscible. The apparent contradiction between our results and those of Lemieux and Prud'homme[18] is likely to be a result of molecular weight and polydispersity differences between samples as well as differences in blend composition.

Once again, at T_{ann} = 383 K, two transitions, at 374 and 406 K, were observed (Figure 4). The breadths of these transitions are 41 and 8 K, respectively (Table 3). The second transition at 406 K was attributed to the decomplexation of complexed sections formed during scanning by Schomaker and Challa.[15] However, one should note that a similar transition was not observed at any other annealing temperatures, which suggests that there may be a low degree of stereocomplexation occurring only at 383 K.

Annealing experiments carried out at higher temperatures, i.e., above 408 K (Figure 4) reveal single T_gs at all annealing temperatures. The relatively large breadth of these transitions compared to those of the pure polymers indicates that these may only be marginally miscible at these temperatures.

4.3. Miscibility Studies of 50/50 iPMMA2/sPMMA. The effect of annealing on the miscibility of 50/50 wt % iPMMA2/sPMMA is shown in Figure 5. T_g and ΔT values (±5% uncertainty) are summarized in Table 4.

At T_{ann} = 313 K, no stereocomplexation takes place, as suggested by the absence of a peak around 463 K. In addition, the blend exhibits two T_gs indicating phase separation of iPMMA2 and sPMMA. Similar results are obtained at 323 and 333 K where again no stereocomplexation takes place and two distinct T_gs are observed. For this system, while T_{g1} is very

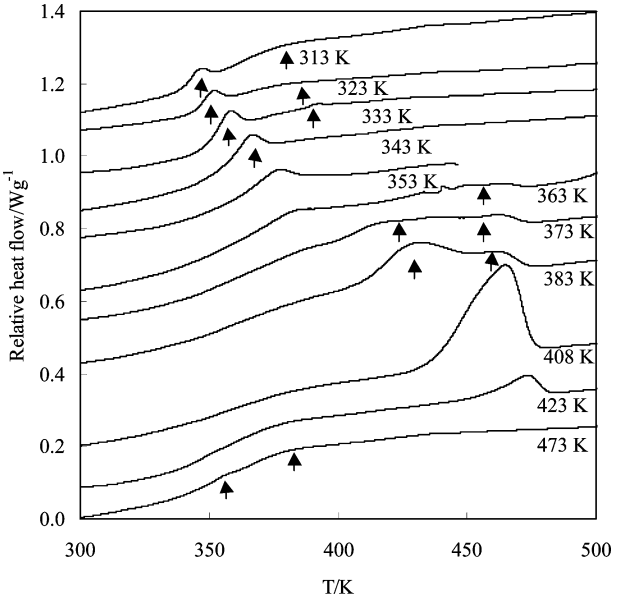

Figure 5. DSC thermograms of 50/50 iPMMA2/sPMMA blends. Each trace is displaced vertically for clarity. Arrows indicate thermal transitions.

Table 4. T_g and ΔT Values Obtained after Annealing the 50/50 iPMMA2/sPMMA Sample

	T_{g1}/K		T_{g2}/K	
T_{ann}/K	T_g	ΔT	T_g	ΔT
313	343	6	363	19
323	348	7	366	14
333	355	9	389	5
343	362	10		
353	370	16		
363[a]	374	28		
373[a]	406	41		
383[a]	356	30		
408[b]				
423	347	35		
473	353	10	367	13

[a] Stereocomplexation occurs and is followed by lamellar crystallization while increasing annealing temperatures from 363 to 408 K.[15] [b] Melting of lamellarly crystallized stereocomplexes at 463 K (peak maximum).

pronounced, T_{g2} is not well-defined, but a small transition around 390 K can be detected. Moreover, the T_g values move closer together when T_{ann} increases from 313 to 333 K. The breadth of T_{g2} decreases upon annealing from 19 to 5 K whereas values for T_{g1} increase from 6 to 9 K. These results suggest slow diffusion of sPMMA into iPMMA and hence miscibility between the two polymers increases gradually when increasing T_{ann} from 313 to 333 K.

Unlike the iPMMA1/sPMMA blend, a single phase was observed for iPMMA2/sPMMA at $T_{ann} = 343$ K, with a single T_g at 362 K ($\Delta T = 10$ K). This is in good agreement with the calculated T_g value (367 K) using the Flory−Fox[31] eq 8. At $T_{ann} = 353$, even though a slight broadening of the iPMMA2/sPMMA glass transition is evident ($\Delta T = 16$ K), the system is still one-phase. When T_{ann} reaches 363 K, the observed single T_g is broader ($\Delta T = 28$ K) than at lower annealing temperatures, suggesting a marginal miscibility of iPMMA2 with sPMMA. Moreover, a broad endothermic peak is observed around 450 K, indicating the melting of stereocomplexed sections of the polymer chains.[15] Here again the observed miscibility behavior is in contradiction with the Lemieux and Prud'homme[18] annealing experiments.

As shown in Figure 5, annealing at and above 373 K causes a broadening of the T_g and appearance of two overlapping

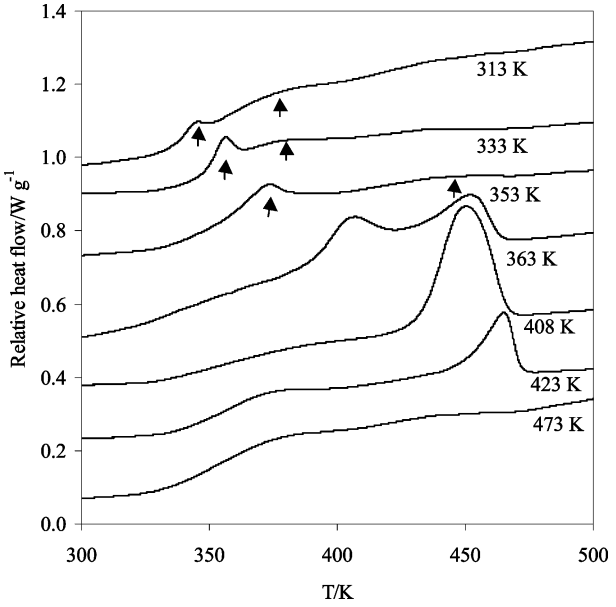

Figure 6. DSC thermograms of 50/50 iPMMA3/sPMMA blends as a function of annealing temperature. Arrows indicate thermal transitions. Each trace is moved vertically for clarity.

Table 5. T_g Values after Annealing a iPMMA3/sPMMA (50/50 wt %) Sample

	T_{g1}/K		T_{g2}/K	
T_{ann}/K	T_g	ΔT	T_g	ΔT
313	341	8	359	19
333	353	8	371	6
353	366	20		
363[a]				
408[b]				
423	360	29	*c*	
473	355	38		

[a] Stereocomplexation followed by lamellar crystallization occurs, peak maxima are at 407 and 449 K, respectively. [b] Lamellar crystallization occurs, which melt at 449 K. [c] Lamellar crystallization occurs, melting observed at 460 K.

endothermic peaks in the region 425−460 K. Using a mechanistic model, Schomaker and Challa[15] identify these two endotherms with (a) the decomplexation of sections partly organised into fringed-micellar clusters (for $T_m = 430$ K) and (b) the simultaneous decomplexation and melting of lamellarly crystallized complexes (for $T_m = 463$ K).

At $T_{ann} = 408$ K, the T_g is almost undetectable and a strong endothermic peak is observed at ∼463 K due to melting of stereocomplexes. As indicated by Schomaker and Challa,[15] at low annealing temperatures ($T_{ann} = 373$ and 383 K), the rate of complexation is faster than the subsequent crystallization and this results in an endotherm around 430 K. At higher annealing temperature, ($T_{ann} = 408$ K) lamellar crystallization occurs directly and is observed as an endothermic peak at 463 K.

Further annealing at 423 K leads to a broad glass transition ($\Delta T = 35$ K) and comparatively small endothermic peak around 463 K whereas at 473 K, the DSC trace shows evidence of two glass transitions, indicating phase separation of iPMMA2 and sPMMA.

4.4. Miscibility Studies of 50/50 iPMMA3/sPMMA. Annealing experiments for the 50/50 wt % iPMMA3/sPMMA sample were carried out in the temperature range 313−473 K and the DSC traces are shown in Figure 6 while T_g and ΔT values are reported in Table 5.

As observed for the other blends, the miscibility behavior and stereocomplex formation are highly dependent upon the

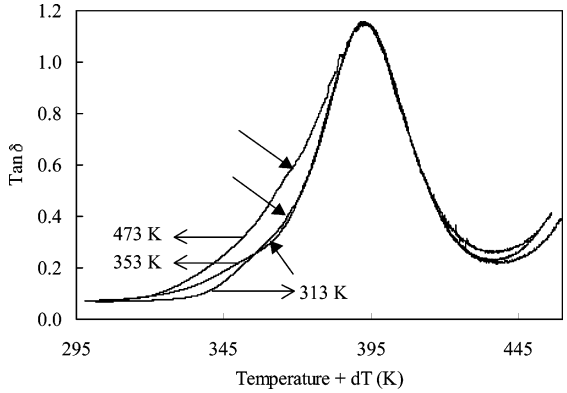

Figure 7. tan δ as a function of annealing temperature for 50/50 iPMMA2/sPMMA. Data have been normalized and shifted horizontally by an amount dT equal to the T_g difference, to overlap the peaks. Arrows indicate the presence of shoulders and differentiate between data at different T.

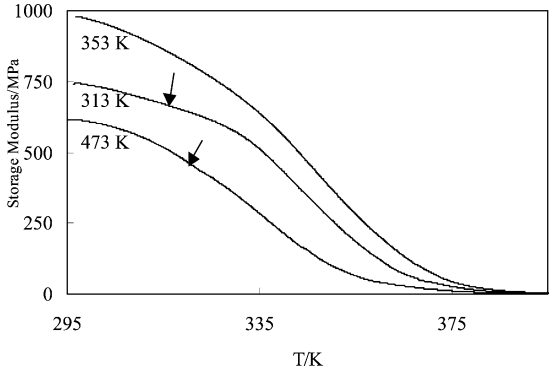

Figure 8. Storage modulus as a function of temperature for 50/50 iPMMA2/sPMMA. Arrows indicate the presence of shoulders.

annealing temperature. At low T_{ann}, two glass transitions are observed indicating immiscibility up to 333 K for this blend system. As mentioned for the other blends, the two T_gs move closer together with increasing T_{ann} and changes in ΔT values associated with T_{g2} are observed.

This blend is miscible at 353 K, although the single T_g is associated with a ΔT value (20.2), which is higher than that of the individual PMMA components. Moreover, the observation of a small shoulder locates the onset of stereocomplexation between iPMMA3 and sPMMA at 450 K.

At $T_{ann} = 363$ K, the T_g is almost undetectable and the two melting peaks at 407 and 450 K indicate formation of stereocomplexes followed by crystallization.[15] For iPMMA1/sPMMA and iPMMA2/sPMMA, no melting peaks were observed upon annealing at 363 K. This apparent contradiction is a result of differences between the molecular weights of the iPMMA samples used and our DSC results indicate that low molecular weight iPMMA enhances the formation of stereocomplexes between iPMMA and sPMMA.[15]

At $T_{ann} = 408$ K, similar to iPMMA2/sPMMA, the T_g becomes undetectable due to lamellar crystallization of stereocomplexed iPMMA3/sPMMA while a broad glass transition ($\Delta T = 29$ K) is evident at 423 K alongside a small endothermic peak at $\sim$ 450 K. Finally when the sample is annealed at 473 K, a single, broad T_g is clearly observed indicating once again a low degree of miscibility between iPMMA3 and sPMMA.

4.5. DMTA Measurements on iPMMA2/sPMMA. The annealing experiments described in the previous sections do suggest that iPMMA1, iPMMA2, and iPMMA3 are miscible with sPMMA over a relatively narrow temperature range around 350 K. All the 50/50 wt % blends appear to be phase separated for $T_{ann} \leq 340$ K, while for $T_{ann} \geq 360$ K, in the iPMMA samples, the increased width of the blend glass transition suggests an increased level of microheterogeneity in the system. This in turn appears to indicate that the iPMMA samples are marginally miscible with sPMMA at these temperatures.

To confirm these results, DMTA experiments on 50/50 iPMMA2/sPMMA were carried out. Three representative annealing temperatures, i.e., 313, 353, and 473 K, were selected, corresponding to samples which were found to be immiscible, miscible, and then again immiscible by the DSC measurements.

Figures 7 and 8 show plots of the loss factor (tan δ) and storage modulus as a function of annealing temperature. The blend sample annealed at 353 K displays a tan δ peak at 392 K (corresponding to the tan δ maximum), whereas the samples annealed at 313 and 473 K show main tan δ peaks at 388 and 384 K, respectively. Close inspection of the tan δ and storage modulus traces, reveal the presence of additional processes, evidenced as a shoulder to the main tan δ peak, around 350 K. This is attributed to a relaxation process associated with the glass transition of iPMMA2. However, the intensity of this shoulder is comparatively less for the sample annealed at 353 K (Figure 7). The storage modulus as a function of temperature shows additional processes for the samples annealed at 313 and 473 K (Figure 8). All these results support the conclusion from the DSC measurements that iPMMA2 is more miscible with sPMMA at 353 K than at 313 and 473 K.

4.6. Calculated Phase Diagrams of iPMMA/sPMMA Blends. Calculations of phase diagrams were also carried out for iPMMA/sPMMA blends using the model described in section 3. Various parameters are required to obtain the theoretical phase behavior and these are listed in Table 6. The molar volumes refer to experimental values while solubility parameters are calculated using the group contribution method of Small.[32] The length of the statistical skeletal units, $\langle l_v \rangle$, equal those previously determined by Wu.[29]

For the iPMMA/sPMMA system, the temperature dependence of the conformational changes as described by d(ln C_∞)/dT has been incorporated into the model.[33] Many authors have reported values of unperturbed dimensions for stereoregular PMMAs. For example, C_∞ values derived from SANS experiments are available in the literature. Other literature values are also listed in Table 6 and are discussed below.

Using small and intermediate angle neutron scattering, Reilly et al.[34] reported C_∞ values of 10.7 and 9.2 for isotactic and syndiotactic PMMAs, respectively. The C_∞ value of iPMMA is in very good agreement with that measured by Jenkins and Porter[35] ($C_\infty = 10.2$) from solution measurements carried out using a GPC coupled with an on-line low angle laser light scattering photometer. However, the same authors reported a lower value of 7.3 for sPMMA. Unperturbed dimensions were obtained by means of viscosity plots and the authors concluded that isotactic PMMA is 30% more extended than syndiotactic PMMA, in its unperturbed state. By performing conformational energy calculations, Sundararajan and Flory[33,36] found C_∞ values that were within the range of the experimental ones, i.e., 9.2−10.7 for iPMMA and 7.3−8.4 for sPMMA, as reported by Sakurda et al.[37] and Schulz et al.,[38] respectively.

As mentioned earlier, Wu[29] developed a method to predict C_∞ values from the polymer chemical structure, using group additivity. For stereoregular PMMAs, the predicted C_∞ values are 10.6 for iPMMA and 8.1 for sPMMA, in agreement with results of Jenkins and Porter.[35]

Overall, for iPMMA, SANS, solution measurements and calculations are in good agreement, giving similar C_∞ values.

Table 6. Parameters Used for the Calculations of Phase Diagrams of iPMMA/sPMMA Blends

polymer	V (cm^3/mol)	δ (cal/cm^3)$^{0.5}$	$\langle l_v \rangle$ (Å)	C_∞	d(ln C_∞)/dT	refs
iPMMA	85.6	8.9	1.53	10.7	−0.0023	29, 32, 34, 37
sPMMA	85.6	8.9	1.53	9.2	0.0014	29, 32, 34, 37

Table 7. C_∞ Values and Their Temperature Dependence for PMMA Stereoisomers

polymer	C_∞	method	d(ln C_∞)/dT × 10^3	method
iPMMA	10.7	neutron scattering[34]	−2.3	solution experiments[37]
	10.2	solution experiments[35]	−0.9 to −1.5	calculation[36]
	9.2 −10.7	solution experiments[37,38]		
	10.6	group contribution[29]		
sPMMA	9.2	neutron scattering[34]	0[a]	solution experiments[39]
	7.3	solution experiments[35]	1.4	solution experiments[39]
	7.3−8.4	solution experiments[37,38]	2.4	solution experiments[38]
	7.2	group contribution[29]	4.0	solution experiments[40]

[a] For conventional PMMA, i.e., 80% sPMMA.

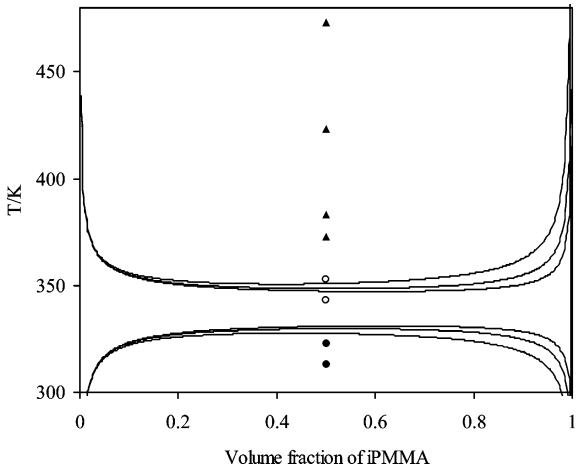

Figure 9. Phase diagrams of iPMMA/sPMMA blends; decreasing iPMMA molecular weight from 300 to 48 × 10^3 g mol^{-1} leading to broadening of the miscibility gap in iPMMA/sPMMA blends. Experimental results from 50/50 iPMMA2/sPMMA blends are included (● is immiscible, ○ is miscible, and ▲ is partially miscible regions).

A greater variation among C_∞ values from different techniques can be noted for the syndiotactic PMMA. In this case, we have selected the SANS value, which should provide an accurate measure of polymer conformation.

The reported temperature dependence of C_∞ for isotactic and syndiotactic PMMA is also given in Table 7. For isotactic PMMA, the temperature coefficient has been found to be negative, whereas it is positive for the syndiotactic chains. Comparison between experimental and calculated C_∞ values clearly indicates that the temperature coefficients for both the isotactic and syndiotactic chains may vary widely. The calculations to be reported here are based on the experimental temperature dependence of C_∞ reported by Sakurda et al.[37]

The temperature dependence of C_∞ is incorporated into the model through the Kuhn segment length, which is given by

$$b_k = \langle l_v \rangle \times e^{[d(\ln C_\infty)/dT(T-T_{ref})]} \quad (9)$$

where T_{ref} is the reference temperature (in this case, e.g., 298.15 K). Using eq 9, the Kuhn segment length can be calculated for the two polymers, as a function of temperature. By substituting into eq 7, one can then evaluate the surface to volume ratio of the individual polymers, from which the temperature coefficient of the interaction parameter can be obtained.

Figure 9 shows the predicted phase behavior for iPMMA1/sPMMA, iPMMA2/sPMMA, and iPMMA3/sPMMA blends. The model clearly reproduces the main feature of the iPMMA/sPMMA in that it displays both upper and lower critical solution temperatures. Moreover, the model predicts that miscibility of iPMMA and sPMMA should be limited to a narrow temperature range around 350 K. In other words, the incorporation of the temperature dependence of C_∞ is responsible for the appearance of two critical temperatures (UCST and LCST) in the blend phase diagram.[33]

To the best of our knowledge, this is the first time that a solubility parameter type model has been utilized to predict an LCST without employing an equation of state approach. It is also encouraging to note that the model reproduces the temperature range over which blend miscibility is occurs reasonably well.

5. Conclusions

In agreement with other studies reported in the literature, annealing experiments at 408 K indicate that formation of stereocomplexes between iPMMA and sPMMA is molecular weight dependent. The low and medium molecular weight iPMMA samples used here formed stereocomplexes with sPMMA. However, for the high molecular weight iPMMA sample, stereocomplexation with sPMMA required very long annealing times, 3−14 days.

A series of annealing experiments showed that the miscibility of iPMMA with sPMMA gradually increased with increasing annealing temperature from 313 to 343 K, completely miscibility being observed around 340−350 K.

A simple model has been proposed which provides an extension to the Flory−Huggins theory as it incorporates Staverman's ideas introduced for small molecules into a polymer theory. We have shown that experimentally determined phase diagrams and calculations are in good agreement. By accounting for the temperature dependence of C_∞ it has been possible to reproduce the main feature of the experimental data that is the presence of two critical temperatures (UCST and LCST). Moreover, calculations indicate that a decrease of the iPMMA molecular weight from 300 to 48 × 10^3 g mol^{-1}, should lead to widening of the miscibility gap.

The annealing experiments have suggested that the optimum temperature to observe miscibility between iPMMA1 and sPMMA is around 350 K. This is molecular weight dependent, and for the iPMMA2/sPMMA sample, it is located at 340−350 K.

The calculated phase diagrams reported in Figure 9 also indicate that the blend should be immiscible above 360 K. However, annealing experiments show a low degree of miscibility or partial miscibility when the iPMMA/sPMMA samples are annealed above 360 K. Such a discrepancy between

experiments and calculations is perhaps not surprising. The theoretical model accounts for packing effects in a system where only dispersive interactions are active between components. For iPMMA/sPMMA blends, miscibility is due to both specific and dispersive interactions, since the polymers possess polar groups. Despite this discrepancy, it is perhaps remarkable that such a simple model is able to reproduce all the relevant feature of this complex system.

Acknowledgment. This work received funding from DSM. L.R. gratefully acknowledges financial support from Heriot-Watt University and the award of an Overseas Research Scholarship. The authors thank Professor Dame Julia S. Higgins for kindly donating the sPMMA sample.

References and Notes

(1) Maier, R. D.; Thomann, R.; Kressler, J.; Mulhaupt, R.; Rudolf, B. *J. Polym. Sci., Part B: Polym. Phys.* **1997**, *35*, 1135.
(2) Phillips, R. A. *J. Polym. Sci., Part B: Polym. Phys.* **2000**, *38*, 1947.
(3) Silvestri, R.; Sgarzi, P. *Polymer* **1998**, *39*, 5871. Phillips, R. A.; Jones, R. L. *Macromol. Chem. Phys.* **1999**, *200*, 1912.
(4) Ermer, H.; Thomann, R.; Kressler, J.; Brenn, R. *Macromol. Chem. Phys.* **1997**, *198*, 3639.
(5) Hong, B. K; Jo, W. H.; Kim, J. *Polymer* **1998**, *39*, 3753.
(6) Woo, E. M.; Wu, F. S. *Macromol. Chem. Phys.* **1998**, *199*, 2041. Woo, E. M.; Lee, M. L.; Sun, Y. S. *Polymer* **2000**, *41*, 883.
(7) Ragupathy. L.; Arrighi, V.; Kraft, A.; McEven, I. J.; Ferguson, R.; Tanchawanich, Z. *J. Polym. Sci., Part B: Polym. Phys.* (submitted).
(8) Krause, S.; Roman, N. *J. Polym. Sci., Part A* **1965**, *3*, 1631.
(9) Bauer, R. G.; Bletso, N. C. *Polym. Prepr. (Am. Chem. Soc., Div. Polym. Chem.)* **1969**, *10*, 632.
(10) Schroeder, J. A.; Karasz, F. E.; Macknight, J. *Polymer* **1985**, *26*, 1795.
(11) Liquori, A. M.; Anzuino, G.; Coiro, V. M.; D'Alagni, M.; de Santis, P.; Savino, M. *Nature (London)* **1965**, *206*, 358.
(12) Challa, G.; de Boer, A.; Tan, Y. Y. *Int. J. Polym. Mater.* **1976**, *4*, 239.
(13) Bosscher, F.; Keekstra, D.; Challa, G. *Polymer* **1981**, *22*, 124.
(14) Feitsma, E. L.; de Boer, A.; Challa, G. *Polymer* **1975**, *16*, 515.
(15) Schomaker, E.; Challa, G. *Macromolecules* **1988**, *21*, 2195.
(16) Katime, I.; Quintana, J. R.; Veguillas, J. *Eur. Polm. J.* **1985**, *21*, 1075.
(17) Schomaker, E.; ten Brinke, G.; Challa, G. *Polymer* **1986**, *27*, 256.
(18) Lemiux, E. J.; Prud'homme, R. E. *Polymer* **1998**, *39*, 5453.
(19) Staverman, A. J. *Rec. Trav. Chim.* **1937**, *56*, 885.
(20) Utracki, L. A. *Polymer Alloys and Blends: Thermodynamics and Rheology*; Hanser Publishers: Munich, Germany, 1990; Chapter 1, p 34.
(21) Painter, P. C.; Veytsman, B.; Kumar, S.; Shenoy, S.; Graf, J. F.; Xu, Y.; Coleman, M. M. *Macromolecules* **1997**, *30*, 932−942.
(22) Londono, J. D.; Maranas, J. K.; Mondello, M.; Habenschuss, A.; Grest, G. S.; Debenedetti, P. G.; Graessley, W. W.; Kumar, S. K. *J. Polym. Sci., Part B: Polym. Phys.* **1998**, *36*, 3001−3005.
(23) Sanchez, I. C.; Lacombe, R. H. *Macromolecules* **1978**, *11*, 1145.
(24) Sanchez, I. C.; Balaz, A. C. *Macromolecules* **1989**, *22*, 2325.
(25) Hildebrand, J. H. *The solubility of nonelectrolytes*; Dover Publications: New York, 1964.
(26) Beckman, E. J.; Hoefling, T. A.; Van Opstal, L.; Koningsveld, R.; Porter, R. S. *Fluid Phase Equilib.* **1994**, *87*, 1833.
(27) Helfand, E.; Sapse, A. M. *J. Chem. Phys.* **1975**, *62*, 1327.
(28) Wu, S. *J. Polym. Sci., Polym. Phys.* **1989**, *27*, 723.
(29) Wu, S. *Polym. Eng. Sci.* **1992**, *32*, 823.
(30) Wang, Z. G. *Macromolecules* **1995**, *28*, 570−576.
(31) Fox, T. G. *Bull. Am. Phys. Soc.* **1953**, *1*, 123.
(32) Krevelen, V.; Hoftyzer, P. J. *Properties of Polymers*; Elsevier Publishing Company: Amsterdam, 1972.
(33) Sundararajan, P. R.; Flory, P. J. *J. Am. Chem. Soc.* **1974**, *96*, 5025.
(34) O'Reilly, J. M.; Teegarden, D. M.; Wignall Wignall, G. D. *Macromolecules* **1985**, *18*, 2747.
(35) Jenkins, R.; Porter, R. S. *Polymer* **1982**, *23*, 105.
(36) Sundararajan, P. R. *Macromolecules* **1986**, *19*, 415.
(37) Sakurda, I.; Nakajima, A.; Yoshizaki, O.; Nakame, K. *Kolloid, Z.* **1962**, *41*, 186.
(38) Schulz, G. V.; Wunmderlich, W.; Kirste, R. *Makromol. Chem.* **1964**, *22*, 75.
(39) Fox, T. G. *Polymer* **1962**, *3*, 111.
(40) Moore, W. R.; Fort, R. F. *J. Polym. Sci., Part A* **1963**, *1*, 929.
(41) Biros, J.; Maasa, Z.; Pouchly, J. *Eur. Polym. J.* **1974**, *10*, 629.

MA061627Q